Journal of King Saud University – Science 35 (2023) 102687

HOSTED BY

Contents lists available at ScienceDirect

Journal of King Saud University – Science

journal homepage: www.sciencedirect.com

Original article

Cytotoxicity and Antimicrobial efficiency of gold (Au) nanoparticles formulated by green approach using *Andrographis paniculata* leaf extract

Viji Paramasivam [a], Prema Paulpandian [a,*], Karthikeyan Venkatachalam [b], Shahid Hussain [c], Aleyna Kangal [d], Dunia A. Al Farraj [e], Mohamed S. Elshikh [e], Paulraj Balaji [f,*]

[a] *Department of Zoology, VHN Senthikumar Nadar College, Virudhunagar, Tamilnadu, India*
[b] *Faculty of Innovative Agriculture and Fishery Establishment Project, Prince of Songkla University, Surat Thani Campus, Makham Tia, Mueang, Surat Thani 84000, Thailand*
[c] *School of Materials Science and Engineering, Jiangsu University, Zhenjiang 212013, China*
[d] *School of Arts and Sciences, New Brunswick-Piscataway Area campus of Rutgers University, USA*
[e] *Department of Botany and Microbiology, College of Science, King Saud University, P.O. 2455, Riyadh 11451, Saudi Arabia*
[f] *PG and Research Centre in Biotechnology, MGR College, Hosur, Tamilnadu, India*

ARTICLE INFO

Article history:
Received 21 May 2022
Revised 5 April 2023
Accepted 11 April 2023
Available online 18 April 2023

Keywords:
Gold nanoparticles
Andrographis paniculata
Antibacterial
Antifungal
Cytotoxicity

ABSTRACT

Gold (Au) nanoparticles have flourished a promise for solicitations in biology due to their processability and high performance in the release of therapeutics. The use of leaf substances in the fundamental biosynthesis and manufacturing of nano-phytomedicine is the cooperative effort between plant science and nanotechnology, yielding a green nanostructured material. This study aims to synthesize AuNPs using the extract taken from *Andrographis paniculata* leaves and to evaluate its efficacy against MCF7 cells and chosen human pathogens. AP-AuNPs were studied with UV, FTIR, and X-ray diffraction spectroscopy, SEM and TEM (scanning and transmission electron microscopy). At 533 nm, a peak of Surface Plasmon Resonance (SPR) was identified using UV–Visible spectra of AuNPs. The XRD diffraction peaks indicated the crystalline nature of gold nanoparticles. The spherical shape was demonstrated by transmission electron microscopy, and dynamic light scattering using Particle Size Analyzer measurements revealed a mean particle size of 40 ± 18.6 nm. The research concluded that using gold nanoparticles derived from herbs is contingent on safe dosage and precise formulation, as stated in ancient literature. MCF7 human breast cancer cells have been used to evaluate the anti-proliferative activity of AuNP. The findings of an oncology investigation revealed that treating cancerous cells using AuNPs drastically diminished the viability of cells. The anti-microbial properties in the primordial herbal-based metal nanoparticles confess the conventional healthcare practice as a progressive approach for contemporary conditions. Based on the investigation, the study inferred that AP-AuNPs are therapeutic in combating human pathogens.

1. Introduction

Emerging technology in nanoscience is essential for the formulation, manufacturing and production of nanostructured materials with diameters range of 1–100 nm in size (Lee et al., 2020). Metal based nanoparticles have significant role in multidisciplinary science and technology owing to its particular characteristics, including a high surface-to-volume ratio, photonic behaviors, surface-enhanced raman resonant frequency, fluorescent combustion, photo-thermal interactions, and perhaps other features of those same nanoparticles have prompted scientists to find and better understand to utilize them in biomedical activities (Borse et al., 2020). Plant material-based nanoparticle formulation has expected a lot of attentiveness in current epochs due to its enormous improvements over additional techniques of nanoparticle development. It overtures a number of advantages, including usage of ecologically sustainable substances and benign compounds (Tejasvi et al., 2021). In contrast to conventional approaches that have used detergents and volatile compounds as reductant, this methodology employs natural molecules such as phytonutrients for example alkaloids, phenolic compounds, corticosteroids, and polypeptides

* Corresponding authors.
E-mail addresses: prema.drprema@gmail.com (P. Paulpandian), balaji_paulraj@yahoo.com (P. Balaji).
Peer review under responsibility of King Saud University.

Production and hosting by Elsevier

https://doi.org/10.1016/j.jksus.2023.102687
1018-3647/

as reductants to transform metal ions into nanostructured materials (Karthik et al., 2020). As a result, fabrication by green approach could be regarded as an alternate method for producing nanocomposites quickly and safely. Gold (Au) nanoparticles have recently garnered a pronounced consideration owing to the breadth of immense uses in biomedicines, biosensor, therapeutic agents, biopharmaceuticals, and biological engineering (Lydia et al., 2020).

Breast cancer remains the second highest prevailing type of cancer worldwide, around 20 lakhs new occurrences reported annually. Cancer disease morbidity seems to be on the increasing around the world, because there are no better therapies or surgeries (Shunmugam et al., 2021). Traditional chemotherapy drugs are not always detrimental to health, but they are also expensive (Brenner et al., 2020). Towards this premise, less expense and healthier techniques of strengthening anticancer medications and treatments are critical. The derivatives of herbal source utilized in the green based formulation of nanoparticles may improve their biologic capability. Green synthesized AuNPs are extensively elucidated for their biological potentialities like microbial killing and cytotoxic efficacy, whereas the gold nanoparticles are still feebly characterized for their biomedical functions. Few previous studies have revealed the effectiveness of AuNPs produced by *Dunaliella salina* and Dragon fruit plants towards breast cancer cells of human (Divakaran et al., 2019). Earlier reports described dosage relevant anticancer effect of AuNPs synthesised get through a plant source as a reducing agent against lung and bladder cancer cells (Wu et al., 2019). Hence, MCF7 cell lines was chosen to evaluate the anticancer potentialities using the phyto mediated synthesis of AuNPs in this work.

Infections caused by microorganism are an antibiotic resistant through the sufficient use of anti-microbial drugs. Microflora of diversified groups are acquiring confrontation to presently accessible antibiotics, pretending a grave hazard to the society. Antimicrobial drugs are unsuccessful in remedying diseases triggered by antibiotic resistant microbes. That kind of anti-microbial drug resistance requires a powerful substitute cocktail (Adil et al., 2019). Herein, a better requirement aimed at unique bactericidal agent designated to circumvent a risk to community hygiene. Subsequently, it is dangerous to generate more effective and affordable technology to fabricate curative mediators to fight against the above-mentioned physical conditions. Green nano tools is an empower solutions to be created using the available resources. Gold nanoparticles have an inspired attention among occurring nanomaterials due to an inert, oxidation-resistance, which produces its purpose in fascinating nano range techniques and tools (Bindhu and Umadevi, 2014). Due to their enormous advantages like drug transportation, bioimaging, catalytic effect, therapeutic agents and disease diagnosis, gold nanoparticles are the utmost intensively developed nanoparticles of all metallic element (Sathiyaraj et al., 2021).

Andrographis paniculata is a herbaceous plant utilized throughout several regions of Southeast Asia for medicinal purposes. It is amongst the most extensively utilized therapeutic species in Middle Asian countries, United states, and Africa for treatment of several diseases like carcinoma, types of diabetes, elevated blood pressure, ulcers, skin problems, malarial fever, flu and leprosy. It acts as immunomodulant, liver protective, antidiarrheal, anti-inflammatory, anti-microbial, antihypertensive, antipyretic, and antimalarial (Mishra et al., 2009). According to phytochemical research, *A. paniculata* encompasses a wide range of bioactive components of pharmacological significance, including high quantity of flavonoids, quinoids, xanthones, tannins, alkaloids, and other compounds (Hossain et al., 2014). Phytomedicines generated from plants are less expensive alternative to chemotherapy drugs. For that reason, the current research focuses *Andrographis paniculata* leaf extract mediated gold (Au) nanoparticles which is contemplated to be the innovative part of this study and promote further explore research for the scrutiny of therapeutic capability for an extensive array of breast cancer medical treatments.

2. Experimental methods

Gold (III) chloride trihydrate ($HAuCl_4{\cdot}3H_2O$) with a purity of 99.99% was procured from HiMedia. 1 mM chloroauric acid stock solution preparation involved dissolving 39.383 mg of gold (III) chloride trihydrate in 100 ml Milli Q water (Water Purification System Model Direct-Q3, Bangalore, India). All glassware items used in this experiment was thoroughly rinsed with deionized water before starting the research work.

2.1. Preparation of Andrographis paniculata leaf extract

Fresh *Andrographis paniculata* leaves were collected in the district of Virudhunagar, Tamil Nadu, India, washed thrice in deionised water, and then shade-dried for one week. Using a grinding machine, the dried leaves were crushed and sieved before being kept in a sealed container for subsequent analysis. Extract of leaves was made by heating 10 g of dried fine powdered leaves in 100 ml of Milli-Q water at 100 °C for 20 min. Using Whatman No. 1 filter paper, the resulting slurry was filtered and was refrigerated at 4 °C for further study.

2.2. Green synthesis of AuNPs

AuNPs were formed in a 100 ml beaker by heating 50 ml of 1 mM gold chloride solution to 80 °C for 10 min. The solution was then agitated for 15 min at 90 °C for 400 rpm. Then, 5 ml of 10% (w/v) *Andrographis paniculata* leaf extract was put in a dropwise manner. The reaction solution was held at ambient temperature for 20 min. to monitor for a colour change. Afterwards, the pale-yellow colored reaction mixture was changed to wine red indicated the development of gold nanoparticles. The green synthesized AuNPs was centrifugated at 8000 rpm for 20 min and the top most fluid was drained off. The obtained precipitate was washed multiple times with milli Q water and the content was dried at 50 °C in hot air oven (Hemmati et al., 2019).

2.3. Characterization of gold nanoparticles

The green generated gold nanoparticles' UV–Vis spectrum was measured at 1 nm resolution and de-ionized water as blank using a Shimadzu dual beam spectrophotometer (model UV – 1650 PC) with wavelengths spanning from 200 nm to 800 nm (Mani et al., 2021). FTIR analysis of AuNPs was performed using Fourier transform infra-red spectroscopy with a range of 4000–400 cm^{-1} in Nicolet Impact 400 FT-IR spectrophotometer (Gandhi et al., 2021). The XRD analysis was determined in the scanning mode on an X'pert PROPAN analytical instrument. The resultant diffraction intensities were compared with the standard Joint Committee for Powder Diffraction Standard (JCPDS) files (Rathnakumar et al., 2019). The distribution of crystalline size of AuNPs was determined using a Tecnai F20 super-Twin FEI transmission electron microscope. DLS (Dynamic light scattering) was measured the average size and polydispersity index of green produced AuNPs. The zeta potential of the AP-AuNPs was measured using Zeta sizer-SZ-100 (Horiba, Japan). To obtain a valid result, the dilution of sample was made using milli Q water at 25 °C and injected into appropriate electrode using a 2 ml disposable syringe (Koperuncholan, 2015).

2.4. Anti-microbial activity

The anti-microbial property of AP-AuNPs was assessed against the human infectious microflora, including *Escherichia coli* (gram-negative), *Staphylococcus aureus*, and *Enterococcus faecalis* (gram-positive), as well as two fungus strains, *Aspergillus niger* and *Candida albicans*. The overnight grown pathogens were swabbed on Mueller Hinton Agar (MHA) plates. The AP-AuNPs with two different concentrations (50 and 100 μg/ml) were dispensed into the agar wells in the petri plates made using cork borer. Then the petri plates were kept overnight at 37 °C. The inhibitory zone was assessed and this study was done in five individual replicates. The minimum inhibitory concentration of AP-AuNPs were determined by broth dilution method using 96 well plate. The sample was diluted twofold at various concentrations and maintained overnight at ambient temperature. A reference was maintained with only organisms. Visual examination and ELISA plate reader (ERBA, LisaScan) measurements of optical density (OD) at 630 nm revealed growth. After obtaining a visual assessment, the OD was instantly quantified. The inhibition of growth in the sample loaded wells for each extract dilution was computed using the following formula;

$$\text{Inhibition } (\%) = \frac{OD\ control - OD\ of\ test\ sample}{OD\ of\ control} \times 100$$

2.5. Cell morphology study

The experimental cells (MCF7) were procured from the NCCS (National Centre for Cell Sciences) located in Pune, India. The cells were cultured in Dulbecco's modified Eagles medium for further study (DMEM, Sigma Aldrich, USA). MCF7 cells were cultured in 96 well plate and incubated at 37 °C for 24 h before each well was individually treated with two-fold diluted 5% DMEM (500 μl) at different concentrations of AuNPs (100, 50, 25, 12.5, 6.25 μg) and maintained in triplicates. Non treated wells are considered as control cells. The Olympus CKX41 with Optika Pro5 CCD camera phase contrast microscope was used to determine the cell morphology.

2.6. Cytotoxicity assay

Fifteen milligram (15 mg) of MTT (Sigma, M−5655) was taken in 3 ml of Phosphate Buffered Saline until complete solubilization and filtered through a sterile filter paper and incubated for 24 h. After that, 30 μl of the diluted MTT solution was poured to all wells (both test and control), now the content was agitated gently and incubated in a humidified chamber with 5% CO_2 for 4 h at 37 °C. The top most layer was removed, then 100 μl of MTT solubilization solution was added and mixed well. Then, the absorbance was recorded at 540 nm in ELISA reader as described by Talarico et al. (2004).

The viability of cell in percentage was calculated by means of the following formula:

$$\text{Viability of cell } = (\%) = \frac{OD\ value\ of\ sample}{OD\ value\ of\ control} \times 100$$

2.7. Staining by AO/EtBr

Acridine Orange (AO) and Ethidium Bromide (EtBr) are DNA binding dyes. These two dyes were used for the detection of apoptotic and necrotic cell's morphology. Acridine orange dye is received by viable and non-viable cells and produces green colour fluorescence if it was intercalated into double stranded DNA. The ethidium bromide dye is grasped by non-viable cells and releases red fluorescence due to the intercalation of DNA. The cells were treated with AP-AuNPs at a concentration of 90.62 μg/ml for 24 h, then washed with cold PBS and stained using AO/EtBr (100 μg/ml, w/v) at ambient temperature for 10 min. After staining, the cells were thoroughly washed two times using 1X phosphate buffered saline and observed under fluorescent microscope.

2.8. DNA fragmentation

The AP-AuNPs at 90.62 μg/ml concentration treated MCF7 cells were trypsinized and pelletized by centrifugation at 5000 rpm for 5 min at 4 °C. The harvested DNA was appended in Tris-EDTA buffer and the DNA fragmentation study was determined by agarose gel electrophoresis (AGE). After staining, the gel was envisioned under UV light in the gel documentation instrument.

2.9. Data analysis

Five individual replicates were carried out independently (n = 5) in each experiment and the standard error of mean (Mean ± SEM) for each group was computed. The post hoc tukey test followed by one-way ANOVA was performed to assess the significant difference of mean values and expressed as $p < 0.05$ and $p < 0.001$. IC_{50} values were determined by dose–response curve generated using ED50 PLUS V1.0 software.

3. Results

3.1. Characterization of AuNPs

Fig. 1 a shows the colour change of green synthesized gold nanoparticle from yellow to wine red colour. Fig. 1 b illustrates the UV–Visible spectrum of AP-AuNPs and its intense absorption peak was recorded at 533 nm. Fig. 1c depicts FTIR spectrum obtained from AP-AuNPs revealed that the stretching bands ranged from 3000 to 3800 cm^{-1} which implies the occurrence of O–H vibration denotes the existence of phenolic compounds, flavonoid contents, anthocyanins and benzophenones in the leaf extract. A diminutive peak shift recommends that the C = O group in the leaf extract acts as capping and stabilizing agents for AP-AuNPs. The stretching vibration at 1510.26 cm^{-1} indicates the presence of C = C aromatic groups and the region of 1249.87 cm^{-1} indicates the amine group (C-N). The C-O stretching vibration band appeared at 1082.07 and 1035.77 cm^{-1} in AP-AuNPs. The stretching occurs at 898.83, and 769.60 cm^{-1}which indicates the C–H bending of alkane groups and the peak at 599.86 and 424.12 cm^{-1}.

XRD pattern of the *A. paniculata* mediated gold nanoparticles, which was crystalline in nature and an intense peak proved the structure of AP-AuNPs (Fig. 1d) to be face centered cubic (fcc) nature including 37.07○, 44.25○, 64.97○, and 77.80○ (111, 200, 220 and 311 respectively) and the obtained data was compared with JCPDS file (No. 00–004-0784). The TEM image of AP-AuNPs synthesized is represented in Fig. 1e. It revealed that the AuNPs is well dispersed with the leaf extract which was acting as the crowning agent to discrete the AuNPs from accumulation. The size of the AuNPs was ranged from 10 to 50 nm and most of them were sphere shaped, few were hexangular and trilateral in shape.

Dynamic light scattering is a standardized particle size analyzer detects an average size of AP-AuNPs was 40 nm by a standard deviation of 18.6 nm (Fig. 1f). The z- average of gold nanoparticle was 31.3 nm in the synthesis process with a poly dispersity index of 0.250. The zeta potential of the AP-AuNPs was −51.1 mV (Fig. 1g) with a tremendous stability.

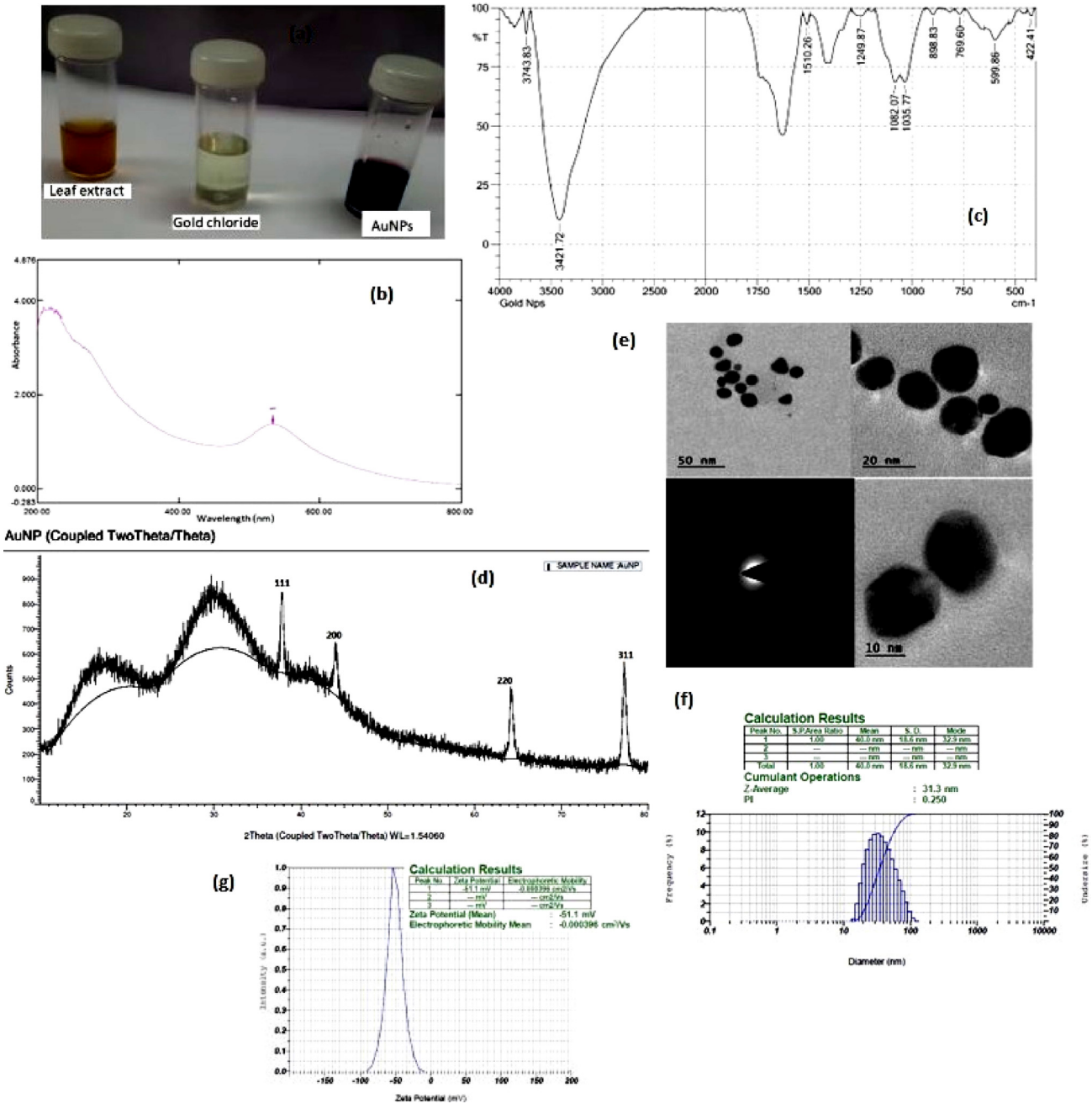

Fig. 1. Characterization of AP-AuNPs: (a) colour change (b) UV (c) FTIR (d) XRD (e) TEM (f) particle size (g) zeta potential.

3.2. Anti-microbial activity

The antibacterial and antifungal efficacy of green synthesized AP-AuNPs was analysed against selected pathogenic microbial strains by agar well diffusion method. The gram positive bacterial strains selected in the study were *S.aureus* and *E.faecalis,* gram negative bacterium *E.coli* and fungal strains such as *A.niger* and *C.albicans*. The observed inhibitory zone is given in Fig. 2. It shows the higher concentration (100 µg/ml) gave better performance than the lower concentration (50 µg/ml). In this lower concentration the fungal strain does not exhibit any zone in the plate. But the standard antibiotic Clotrimazole exhibited better antifungal effect (34 and 26 mm) to *A.niger* and *C.albicans* respectively than the AP-AuNPs (14 and 15 mm) because of the chemical compound exclusively gave increased zone of inhibition. Meanwhile there is no zone of inhibition in the plant extract alone loaded well. The obtained result revealed that the increasing AuNPs concentration gives diminishing growth of microbial cells. The one-way ANOVA test between the low and high concentrations of AP-AuNPs and standard antibiotics such as streptomycin for bacterial strains and clotrimazole for fungal strains showed significant difference ($p < 0.05$) followed by the post hoc tukey test ($p < 0.001$).

Based on these information, the minimum inhibitory concentration (MIC) of the anti-microbial component required to prevent the growth of microflora was found to be 100 µg/ml against *A.niger* and *E.faecalis* (92.13 and 88.74 %) with the respective IC50 values of 15.98 and 15.49 µg/ml. Followed by this, *E. coli* strain was found to be good inhibitory effect (88.18%) at 100 µg/ml with the IC50

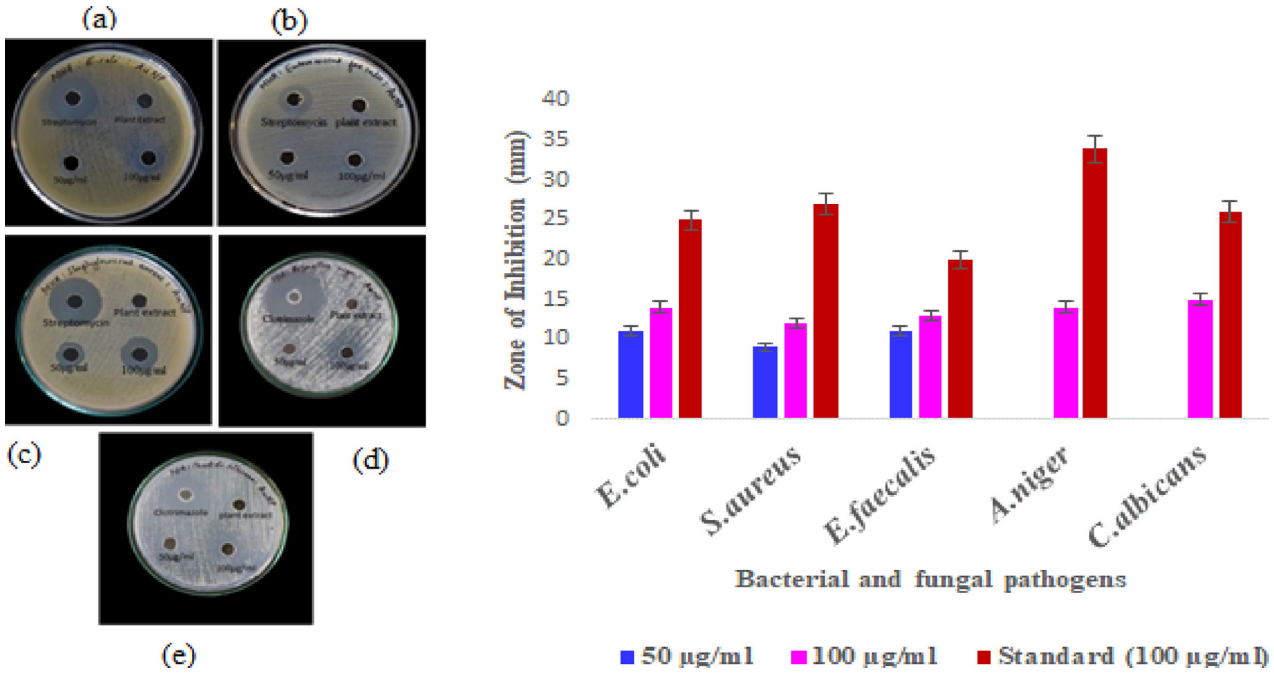

Fig. 2. Antimicrobial activity (inhibition zone in mm) of AP-AuNPs: (a) *E. coli* (b) *E. faecalis* (c) *S.aureus* (d) *A.niger* (e) *C. albicans.*

value (14.57 µg/ml). But more or less similar IC50 values were obtained for *S. aureus* and *Candida albicans* (24.126 and 24.425 µg/ml) respectively (Fig. 3).

3.3. Anticancer study

MTT assay for cytotoxicity efficacy in MCF7 cells was used to determine the effect of AP-AuNPs on breast cancer cell lines. The AP-AuNPs meritoriously decreased MCF7 cell proliferative efficiency from 6.25 µg/ml in a dosage reliant manner ($p < 0.001$) in association through the unprocessed cells. It also explains the normal cell L929 was also used to analyze the proliferative activity using AuNPs for comparative study. It revealed that the greater impact of AuNPs on MCF7 than L929 cells (Fig. 4).

The sigmoidal curve plotted for this dose dependent study of AuNPs on both cells revealed the IC50 value (half maximal) as 90.62 and 159.16 µg/ml. The one-way ANOVA and tukey post hoc test concluded that the proliferative inhibitory action was dose dependent way and each dose differences significantly ($p < 0.001$).

The cell morphology was critically analyzed by means of AP-AuNPs in different dosages. AuNPs treated cancer cells shows significant mortality at increased concentration. The damaged cells were shedding and renovating into an orbicular form. This kind of alteration does not materialize in L929 cell which indicates the experimental AP-AuNPs can inhibit cancer cells via hunting of reactive oxygen species and diminishing oxidative stress and also recommending that it could be expended as curative to skirmish carcinoma cells for anticancer drug development (Fig. 5).

3.4. Apotosis and DNA fragmentation

The apoptosis study using AO/EtBr staining protocol to discriminate the viable and non– viable cells based on the emittance of fluorescence if it intercalated into double stranded DNA. The viable cell emits green and the non– viable cell emits red fluorescence. The present apoptotic result is predicted in Fig. 6. The observed data revealed the living cells are having typical green coloured nucleus, while in the apoptotic cells of early stage form an intense green coloured nucleus with compressed chromatin, the later stage apoptotic cell shows orange coloured stain with fragmentation and damaged (necrotic) cells are homogenously stained as orange red.

AP leaf extract mediated Gold (Au) nanoparticles stimulated programmed cell death which was reliable with the obtained result exhibiting that DNA disintegration take place as seen in Fig. 6. Strength of gold nanoparticles escorted a prolonged tail (DNA damage) supplementary sustaining the event that gold nanoparticles engendered caspase mediated cell death in MCF7 and the recorded information in Fig. 6 shows agarose gel electrophoresis of DNA fragmentation which was improved with intensifying acquaintance to AP-AuNPs. Green synthesized gold nanoparticles demonstrated cellular apoptosis over a diminished cell proliferative action and an improvement in DNA breakup.

4. Discussion

The green synthesis of gold nanoparticle has gained great attentiveness of the researchers due to their plentiful significance in nano -optics, nano sensors, nano-catalysis and nano medicines. Green technology was used to develop gold nanoparticles has numerous applications than using chemical approach because of its ecofriendliness and cost effective. Various plants have emerged as an apparent source for reducing gold chloride precursor in the fabrication of AuNPs. In the present study, *A.paniculata* leaf extract as reducer for the synthesis of AuNPs using precursor salt. The reaction solution colour was altered from yellow to dark red by AuNPs. Similarly, the synthesized gold nanoparticle reaction solution was ruby red colour using *Mentha longifolia* leaf extract (Li et al., 2021). Borse and Konwar, 2020 reported that the colloidal gold nanoparticles were fabricated using tri sodium citrate as reducing agent produced reddish purple colour. The AuNPs prepared using 4 and 5% of *Mucuna monosperma* seed extract exhibited deep purple colour (Vora et al., 2020).

As a result of surface plasmon resonance, gold nanoparticle displays an absorption in the UV–Visible region of an electromagnetic spectrum. Remarkably, the absorption maxima offer facts on the morphological information of the fabricated nanoparticles. The

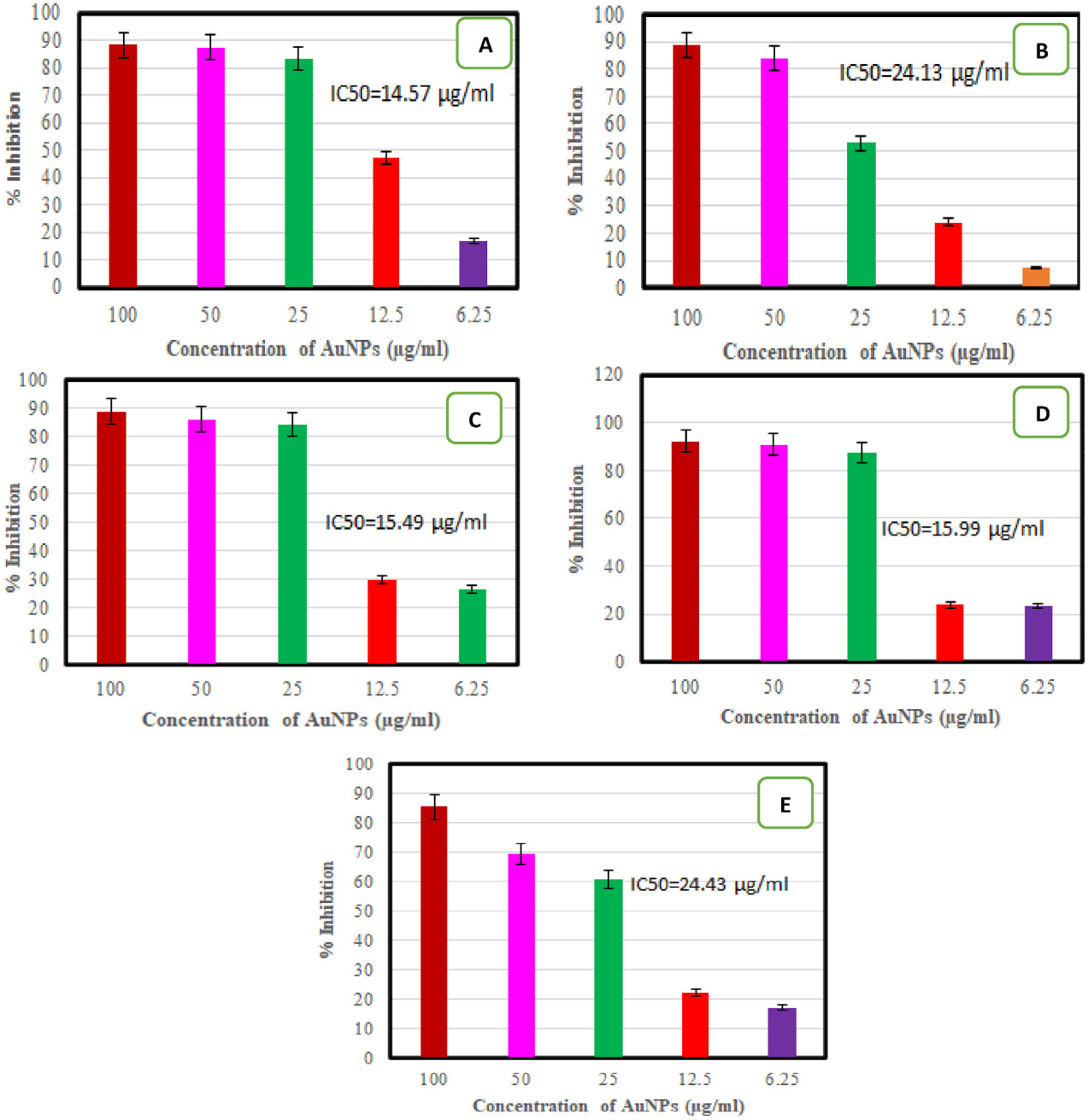

Fig. 3. MIC of AP-AuNPs against bacterial and fungal pathogens (a) *E. coli*, (b) *S. aureus*, (c) *E. faecalis* (d) *A. niger* (e) *C. albicans.*

recorded absorption peak was comparatively lower wavelength at 533 nm in the present experiment with respect to the obtained small sized gold nanoparticle. Previous research, Saqr et al. (2021) demonstrated that sphere-shaped AuNPs overture peak at around 520 nm in the UV–Visible spectrum owing to their adequate and compact size (Saqr et al., 2021). In various studies, the absorption peak of AuNPs was determined at 547 nm (Balasubramanian et al., 2020).

The crystalline nature of *A. paniculata* leaf extract mediated AuNPs was assessed through XRD analysis. Using FTIR, the transmission peaks in the present study were determined to be 3743.83, 3421.72, 1510.26, 1249.87, 1082.07, 1035.77, 898.83, 769.60, 599.86, and 422.41 cm^{-1}, which conforms to research by Nikaeen et al. (2020) and Prema et al (2016). Mahiuddin et al. (2020) attributed the AgNPs synthesized by *Piper chaba* stem extracts showed the vibration at 3447 cm^{-1} ascribed the O–H and N–H groups which implies the crowning of organic molecules present in the extract. The recorded X-ray diffraction data of AP-AuNPs is in accordance with earliet reports (Abdoli et al., 2021). The XRD spectrum of gold nanoparticle synthesized in this investigation revealed the existence of its metallic (Au) constituents, as stated in previous reports (Devanesan and AlSalhi, 2021).

HR-TEM is utilized to establish the accurate size and shape of its crystal-like assembly (Khanna et al., 2019). According to Folorunso et al. (2019), TEM study investigates the size, structure, and particle dispersion of AuNPs and were sphere shaped with a mean size of 37.7 nm. Prema et al. (2022) reported that 80% of the gold nanoparticles synthesized using green tea extract were 20 nm in size. The obtained negative zeta potential value as evidenced due to the presence of negatively charged functional groups in the leaf

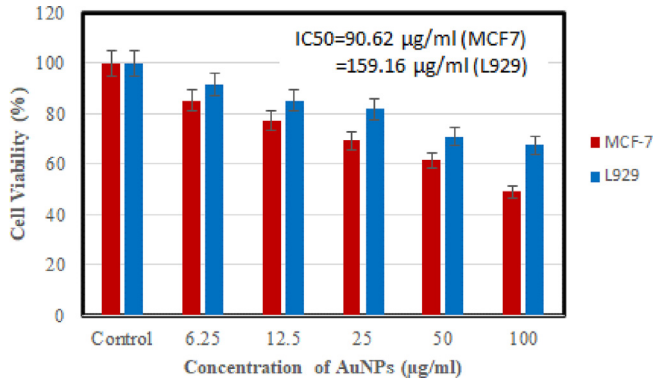

Fig. 4. Cytotoxicity of different concentration of AuNPs (6.25 to 100 µg/ml) from *Andrographis paniculata* against MCF7 and L929 cells.

extract provided the stability of AuNPs. The surface charge of metal-based nanoparticles is either more -ve (30) or more + ve (30), have shown to be more stable (Hemlata et al., 2020).

Metal nanoparticles such as silver and AuNPs (Ni et al., 2018), have been shown to partake good anti-fungal efficiency using *C. albicans* strain and antibacterial properties, particularly those produced using a green technique, but antibacterial effect is reliant on the synthesis process, form, size, and intensity of the prepared AuNPs using green approach (Wani and Ahmad, 2013). They can kill a variety of bacterial pathogens by interacting proactively with them via two main mechanisms: (1) anti-bacterial effect by way of in contact, which happens when nanoparticles adhere to the surface of cell and penetrate it, and (2) ion-mediated death (Vijilvani et al., 2020)(). Prema et al. (2022) revealed that gold nanoparticles fabricated by means of green tea as sole source which excellently declined cell propagation (PC-3) at 10 µg/ml in a dosage reliant manner ($p < 0.001$) when compared by means of cancer cells. Earlier report (Prema et al., 2022) revealed that the morphology of cancer cells shows diminishing effect drastically in a dose dependent way and the cell death was observed in higher doses, as noticed by exterior impassiveness, cell contraction and deformation.

Plant derived substances and nano-based materials have been commended as a favorable and reasonable complementary for remedying MCF7 and other sarcoma cells (Barai et al., 2018). These cytotoxic materials are reducing toxicity and chemical anticipatory, constructing them a flashpoint for tumor research. On the other hand, they are constrained in their proficiency to focus a can-

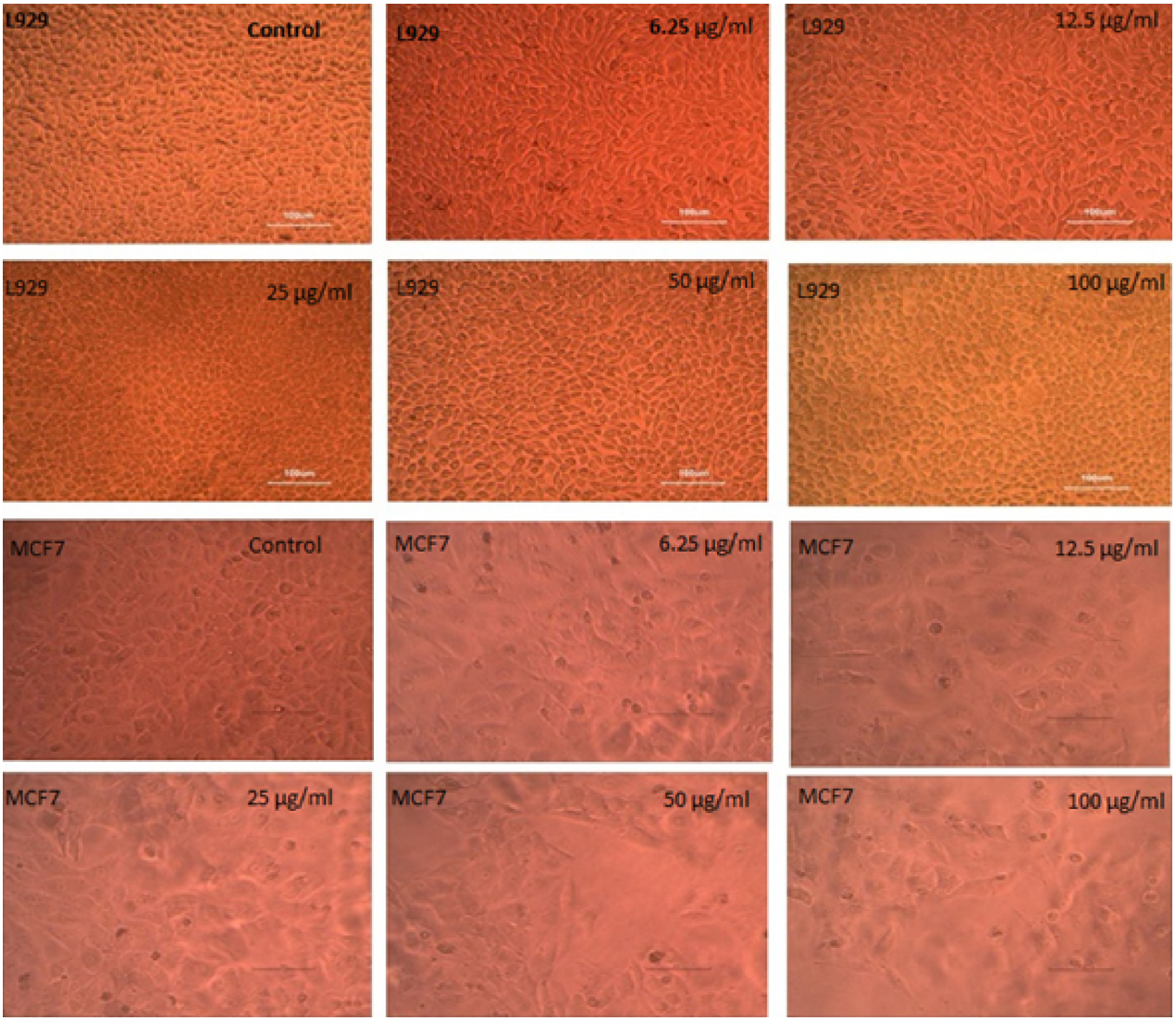

Fig. 5. Image of L929 (normal) and MCF7 (cancer cells) of untreated control and treated with AP-AuNPs.

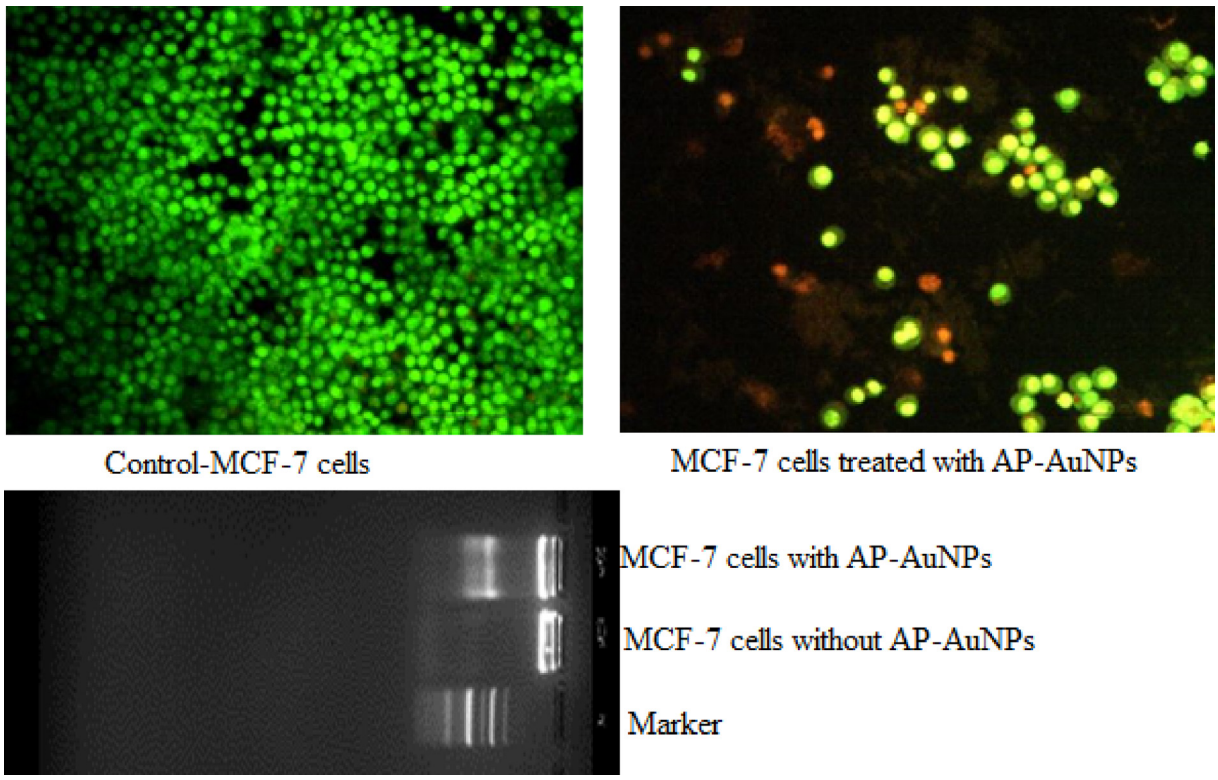

Fig. 6. Apoptosis and DNA fragmentation of MCF7 cells control and treated with AuNPs.

cer position due to disputes like insufficient solubility, organizational distortion and bio accessibility (Manikandakrishnan et al., 2019). For the reason that their highly developed medical uses, gold nanoparticles formulated using seed oil has inspired a plenty of responsiveness in recent days (Oueslati et al., 2020). The provocation of programmed cell death is authorized by two main agents such as diminished and shriveled and DNA disintegration (Sriram et al., 2010). In the present study, AP-AuNPs treated cells indicated caspase mediated cell death in the form of compressed nuclei, membrane blistering and its structural modifications were obvious via AO/EtBr double staining.

The green synthesized gold nanoparticle demonstrated cellular death during the course of cell propagation and an enhanced DNA disintegration. The observed results are synchronized with earlier studies (Datkhile et al., 2021) when we consider DNA fragmentation -stimulated programmed cell death in MCF7 cells subjected to AP-AuNPs. The observed results are concomitant with the previous reports and they contemplated DNA fragmentation stimulated programmed cell death in HCT-15 cells displayed to biogenic *Argemone mexicana* mediated gold nanoparticles (Datkhile et al., 2021). The present results are contemporaneous with the previous studies revealed that the changed cell morphology as well as intensified programmed cell death owing to AM-AuNPs and also substantiated through DNA fragmentation -stimulated cell death in HCT-15 cells subjected to biological mediated AuNPs.

5. Conclusions

The experimental results focused the anti-microbial and anticancer effect of AuNPs synthesized by aqueous leaf extract of *Andrographis paniculata*. The formulated AP-AuNPs were characterized by means of UV–Visible Spectrum, FTIR and XRD spectroscopy, Scanning Electron and Transmission Electron Microscopic analyses. The existence of highly active bioactive green synthesized AP-AuNPs that have anti-microbial efficiency were validated *in vitro* using certain human pathogens. According to the findings, AP-AuNPs is a promising therapeutic agent to combat pathogenic microflora for prospective drug development. It is rational to extrapolate that the pharmaceutic properties of AP-AuNPs offer the anticancer potential for breast cancer causing MCF7 cells. Remarkably, it has been validated that the functionalization of AuNPs as anti-cancer nano drug has been attained without doping any molecules. Present findings markedly authorized the inherent programmed cell death mechanism as a core process involved in apoptosis of MCF7 cells that is highly susceptible to AP-AuNPs.

Declaration of Competing Interest

The authors declare that they have no known competing financial interests or personal relationships that could have appeared to influence the work reported in this paper.

Acknowledgement

The authors thankfully recognize the support rendered by the management of V.H.N. Senthikumara Nadar College in Virudhunagar and MGR College in Hosur, Tamil Nadu, India in performing this study. The authors also extend their appreciation to the Researchers supporting project number (RSP2023R190), King Saud University, Riyadh, Saudi Arabia.

References

Abdoli, M., Arkan, E., Shekarbeygi, Z., Khaledian, S., 2021. Green synthesis of gold nanoparticles using Centaurea behen leaf aqueous extract and investigating their antioxidant and cytotoxic effects on acute leukemia cancer cell line (THP-1). Inorg Chem Commun 129,. https://doi.org/10.1016/j.inoche.2021.108649 108649.

Adil, M., Khan, T., Aasim, M., Khan, A.A., Ashraf, M., 2019. Evaluation of the antibacterial potential of silver nanoparticles synthesized through the interaction of antibiotic and aqueous callus extract of *Fagonia indica*. AMB Express 9. https://doi.org/10.1186/s13568-019-0797-2.

Balasubramanian, S., Kala, S.M.J., Pushparaj, T.L., 2020. Biogenic synthesis of gold nanoparticles using *Jasminum auriculatum* leaf extract and their catalytic, antimicrobial and anticancer activities. J Drug Deliv Sci Technol 57. https://doi.org/10.1016/j.jddst.2020.101620.

Barai, A.C., Paul, K., Dey, A., Manna, S., Roy, S., Bag, B.G., Mukhopadhyay, C. Green synthesis of *Nerium oleander* conjugated gold nanoparticles and study of its in vitro anticancer activity on MCF7 cell lines and catalytic activity Nano Convergence 5(1). https://doi.org/10.1186/s40580- 018-0142-5.

Bindhu, M.R., Umadevi, M., 2014. Antibacterial activities of green synthesized gold nanoparticles. Mater Lett 120, 122–125. https://doi.org/10.1016/j.matlet.2014.01.108.

Borse, V.B., Konwar, A.N., Jayant, R.D., Patil, P.O., 2020. Perspectives of characterization and bioconjugation of gold nanoparticles and their application in lateral flow immunosensing. Drug Deliv Transl Res 10 (4), 878–902. https://doi.org/10.1007/s13346-020-00771-y.

Borse, V.B., Konwar, A.N., 2020. Synthesis and characterization of gold nanoparticles as a sensing tool for the lateral flow immunoassay development. Sensor Int 1,. https://doi.org/10.1016/j.sintl.2020.100051 100051.

Brenner, D.R., Weir, H.K., Demers, A.A., Ellison, L.F., Louzado, C., Shaw, A., Turner, D., Woods, R.R., Smith, L.M. 2020. Projected estimates of cancer in Canada CMAJ 192(9):E199–E205. https://doi.org/10.1503/cmaj.191292. Epub 2020 Mar 2.

Datkhile, K.D., Patil, S.R., Durgawale, P.P., et al., 2021. Biogenic synthesis of gold nanoparticles using *Argemone mexicana* L. and their cytotoxic and genotoxic effects on human colon cancer cell line (HCT-15). J Genet Eng Biotechnol 19 (1), 9–20. https://doi.org/10.1186/s43141-020-00113-y.

Devanesan, S., AlSalhi, M.S., 2021. Green synthesis of silver nanoparticles using the flower extract of *Abelmoschus esculentus* for cytotoxicity and anti-microbial studies. Int. J Nanomed 16, 3343–3356. https://doi.org/10.2147/IJN.S307676.

Divakaran, D., Lakkakula, J.R., Thakur, M., Kumawat, M.K., Srivastava, R., 2019. Dragon fruit extract capped gold nanoparticles: synthesis and their differential cytotoxicity effect on breast cancer cells. Mater Lett 236, 498–502. https://doi.org/10.1016/j.matlet.2018.10.156.

Folorunso, A., Akintelu, S., Oyebamiji, A.K., Ajayi, S., Abiola, B., Abdusalam, I., Morakinyo, A., 2019. Biosynthesis, characterization and anti-microbial activity of gold nanoparticles from leaf extracts of *Annona muricata*. J Nanostruc Chem 9, 111–117. https://doi.org/10.1007/s40097-019-0301-1.

Gandhi, A.D., Kaviyarasu, K., Supraja, N., Velmurugan, R., Suriyakala, G., Babujanarthanam, R., Zang, Y., Soontarapa, K., Almaary, K.S., Elshikh, M.S., Chen, T.W., 2021. Annealing dependent synthesis of cyto-compatible nano-silver/calcium hydroxyapatite composite for anti-microbial activities. Arab J Chem 14. https://doi.org/10.1016/j.arabjc.2021.103404.

Hemlata, Meena, P.R., Singh, A.P., Tejavath, K.K. 2020. Biosynthesis of silver nanoparticles using *Cucumis prophetarum* aqueous leaf extract and their antibacterial and anti-proliferative activity against cancer cell lines. ACS Omega 5(10):5520–5528. https://doi.org/10.1021/acsomega.0c00155.

Hemmati, S., Joshani, Z., Zangeneh, A., Zangeneh, M.M., 2019. Biosynthesis and chemical characterization of polydopamine-capped silver nanoparticles for the treatment of acute myeloid leukemia in comparison to doxorubicin in a leukemic mouse model. Appl Organomet Chem 34 (2), 1–12. https://doi.org/10.1002/aoc.5277 e5277.

Hossain, M.S., Urbi, Z., Sule, A., Hafzur Rahman, K.M. 2014. *Andrographis paniculata* (Burm. f.) Wall ex Nees: A review of ethnobotany, phytochemistry, and pharmacology. Sci World J 2014 http://doi.org/10.1155/2014/274905.

Karthik, C., Suresh, S., Sneha Mirulalini, G., Kavitha, S.A., 2020. FTIR Approach of Green Synthesized Silver Nanoparticles by *Ocimum Sanctum* and *Ocimum gratissimum* on Mung Bean Seeds. Inorg Nano-Met Chem 50, 606–612. https://doi.org/10.1080/24701556.2020.1723025.

Khanna, P., Kaur, A., Goyal, D., 2019. Algae-based metallic nanoparticles: synthesis, characterization and applications. J Microbiol Methods 163,. https://doi.org/10.1016/j.mimet.2019.105656 105656.

Koperuncholan, M., 2015. Bioreduction of chloroauric acid ($HAuCl_4$) for the synthesis of gold nanoparticles (GNPs): A special empathies of pharmacological activity. Int J Phytopharm Res 5, 72–80. https://doi.org/10.7439/ijpp.

Lee, K.X., Shameli, K., Yew, Y.P., Teow, S.Y., Jahangirian, H., Rafiee-Moghaddam, R., Webster, T.J., 2020. Recent developments in the facile bio-synthesis of gold nanoparticles (AuNPs) and their biomedical applications. Int J Nanomed 15, 275–300. https://doi.org/10.2147/IJN.S233789.

Li, S., Al-Minsed, F.A., El-Serehy, H.A., Yang, L., 2021. Green synthesis of gold nanoparticles using aqueous extract of *Mentha longifolia* leaf and investigation of its anti-human breast carcinoma properties in the *in vitro* condition. Arab J Chem 14,. https://doi.org/10.1016/j.arabjc.2020.102931 102931.

Lydia, D.E., Ameer, K., Immanuel, P., Galal, A.E., Naif, A., Mariadhas, V.A., 2020. Photo- activated synthesis and characterization of gold nanoparticles from *Punica granatum* L. seed oil: An assessment on antioxidant and anticancer properties for functional yoghurt nutraceuticals. J Photochem Photobiol B 206,. https://doi.org/10.1016/j.jphotobiol.2020.111868 111868.

Mahiuddin, M., Saha, P., Ochiai, B., 2020. Green synthesis and catalytic activity of silver nanoparticles based on *Piper chaba* stem extracts. Nanomaterials 10 (9), 1777. https://doi.org/10.3390/nano10091777.

Mani, M., Pavithra, S., Mohanraj, K., Kumaresan, S., Alotaibi, S.S., Eraqi, M.M., Gandhi, A.D., Babujanarthanam, R., Maaza, M., Kaviyarasu, K., 2021. Studies on the spectrometric analysis of metallic silver nanoparticles (Ag NPs) using *Basella alba* leaf for the antibacterial activities. Environ Res 199. https://doi.org/10.1016/j.envres.2021.111274.

Manikandakrishnan, M., Palanisamy, S., Vinosha, M., Kalanjiaraja, B., Mohandoss, S., Manikandan, R., Tabarsa, M., You, SangGuan, Prabhu, N.M., 2019. Facile green route synthesis of gold nanoparticles using *Caulerpa racemosa* for biomedical applications. J Drug Deliv Sci Technol 54,. https://doi.org/10.1016/j.jddst.2019.101345 101345.

Mishra, U.S., Mishra, A., Kumari, R., Murthy, P.N., Naik, B.S., 2009. Antibacterial activity of ethanol extract of Andrographis paniculata. Indian J Pharm Sci 71, 436–438. https://doi.org/10.4103/0250-474X.57294.

Ni, Z., Gu, X., He, Y., Wang, Z., Zou, X., Zhao, Y., Sun, L., 2018. Synthesis of silver nanoparticle-decorated hydroxyapatite (HA@ Ag) poriferous nanocomposites and the study of their antibacterial activities. RSC Adv 8, 41722–41730. https://doi.org/10.1039/C8RA08148D.

Nikaeen, G., Yousefinejad, S., Rahmdel, S., Samari, F., Mahdavinia, S., 2020. Central composite design for optimizing the biosynthesis of silver nanoparticles using *Plantago major* extract and investigating antibacterial, antifungal and antioxidant activity. Sci Rep 10 (1), 1–16. https://doi.org/10.1038/s41598-020-66357-3.

Oueslati, M.H., Tahar, L.B., Harrath, A., 2020. Catalytic, antioxidant and anticancer activities of gold nanoparticles synthesized by kaempferol glucoside from *Lotus leguminosae*. Arabian J Chem 13 (1), 3112–3122. https://doi.org/10.1016/j.arabjc.2018.09.003.

Prema, P., Iniya, P.A., Immanuel, G., 2016. Synthesis, characterization, antibacterial and synergistic effect of gold nanoparticles using *Klebsiella pneumoniae* (MTCC-4030). RSC Adv. 6, 4601–4607. https://doi.org/10.1039/C5RA23982F.

Prema, P., Boobalan, T., Arun, A., Rameshkumar, K., Suresh Babu, R., Veeramanikandan Van-HuyNguyen, V., Balaji, P., 2022. Green tea extract mediated biogenic synthesis of gold nanoparticles with potent anti-proliferative effect against PC-3 human prostate cancer cells. Mater Lett 306,. https://doi.org/10.1016/j.matlet.2021.130882 130882.

Rathnakumar, S.S., Noluthando, K., Kulandaiswamy, A.J., Rayappan, J.B.B., Kasinathan, K., Kennedy, J., Maaza, M., 2019. Stalling behaviour of chloride ions: A non-enzymatic electrochemical detection of A-Endosulfan using CuO interface. Sens Actuators B: Chem 293, 100–106. https://doi.org/10.1016/j.snb.2019.04.141.

Saqr, A.A., Khafagy, E.S., Alalaiwe, A., Aldawsari, M.F., Alshahrani, S.M., Anwer, M.K., Khan, S., Lila, A.S., Arab, H.H., Hegazy, W.A.H., 2021. Synthesis of gold nanoparticles by using green machinery: characterization and *in vitro* toxicity. Nanomater 11, 1–14. https://doi.org/10.3390/nano11030808.

Sathiyaraj, S., Suriyakala, G., Dhanesh Gandhi, A., Babujanarthanam, R., Almaary, K.S., Chen, T.W., Kaviyarasu, K., 2021. Biosynthesis, characterization, and antibacterial activity of gold nanoparticles. J Infect Public Health 14 (12), 1842–1847. https://doi.org/10.1016/j.jiph.2021.10.007.

Shunmugam, R., Renukadevi Balusamy, S., Kumar, V., Menon, S., Lakshmi, T., Perumalsamy, H., 2021. Biosynthesis of gold nanoparticles using marine microbe (*Vibrio alginolyticus*) and its anticancer and antioxidant analysis. J King Saud Univ Sci 33, (1). https://doi.org/10.1016/j. jksus.2020.101260 101260.

Sriram, M.I., Kanth, S.B., Kalishwaralal, K., Gurunathan, S., 2010. Antitumor activity of silver nanoparticles in Dalton's lymphoma ascites tumor model. Int J Nanomedicine 5, 753–762. https://doi.org/10.2147/IJN.S11727.

Talarico, L.B., Zibetti, R.G., Faria, P.C., Scolaro, L.A., Duarte, M.E., Noseda, M.D., Damonte, E.B., 2004. Anti-herpes simplex virus activity of sulfated galactans from the red sea weeds Gymnogongrus griffithsiae and Cryptonemia crenulata. Int J Biol Macromol 34 (1–2), 63–71. https://doi.org/10.1016/j.ijbiomac.2004.03.002.

Tejasvi, S., Athira, J., Mohammad, A., Asha, A.M., 2021. Green synthesized gold nanoparticles with enhanced photocatalytic activity. Mater Today 42 (2), 1166–1169. https://doi.org/10.1016/j.matpr.2020.12.531.

Vijilvani, C., Bindhu, M., Princy, F., AlSalhi, M.S., Sabitha, S., Saravanakumar, K., Devanesan, S., Umadevi, M., Aljaafreh, M.J., Atif, M., 2020. Anti-microbial and catalytic activities of biosynthesized gold, silver and palladium nanoparticles from Solanum nigurum leaves. J Photochem Photobiol B 202. https://doi.org/10.1016/j.jphotobiol.2019.111713.

Vora, R.N., Joshi, A.N., Joshi, N.C., 2020. Green synthesis and characterization of gold nanoparticles using *Mucuna monosperma*. J Nanosci Technol 6 (3), 901–904. https://doi.org/10.30799/jnst.309.20060301.

Wani, I.A., Ahmad, T., 2013. Size and shape dependant antifungal activity of gold nanoparticles: a case study of Candida. Colloids Surf B 101, 162–170. https://doi.org/10.1016/j.colsurfb.2012.06.005.

Wu, T., Duan, X., Hu, C., Wu, C., Chen, X., Huang, J., Liu, J., Cui, S., 2019. Synthesis and characterization of gold nanoparticles from Abies spectabilis extract and its anticancer activity on bladder cancer T24 cells. Artif Cells Nanomed Biotechnol 47 (1), 512–523. https://doi.org/10.1080/21691401.2018.1560305.